Progress in Reaction Kinetics and Mechanism, 2018, 43(1), 62–78
https://doi.org/10.3184/146867818X15066862094914 Paper: 1700660

A compact reaction mechanism of methane oxidation at high pressures

Victor P. Zhukov* and Alan F. Kong

Institute of Space Propulsion, German Aerospace Centre (DLR), Langer Grund, 74239 Hardthausen, Germany

**E-mail: victor.zhukov@dlr.de*

ABSTRACT

A skeletal methane kinetic mechanism is developed for conditions relating to the combustion of undiluted methane–oxygen mixtures at high pressures. The new skeletal mechanism is based on the detailed mechanism of oxidation of alkanes by Zhukov (2009). The skeletal model has been created by eliminating unimportant species and reactions from the detailed mechanism. The reduction technique is based on the reaction path and sensitivity analyses. They allow one to determine the reactions and species that play important roles in combustion in rocket combustion chambers. The skeletal mechanism consists of 23 species and 51 reactions. The final and intermediate versions of the skeletal mechanism are compared with the parent detailed mechanism, with other reduced kinetic models and with experimental data on the ignition of methane at high pressures. This comparison shows that the developed skeletal mechanism has a better performance than other kinetic mechanisms in terms of accuracy and required computational power.

KEYWORDS: methane, chemical kinetics, reduced mechanism, high pressure, liquid rocket engine, oxidation of alkanes, free radical, oxygen, flame

1. INTRODUCTION

In the past decade, there has been increasing interest in fuel propellants for in-space and launcher rocket propulsion that reduce the operational cost of launching and improve rocket operating efficiency and performance. Hydrogen provides the best performance in terms of specific impulse at a high cost for the rocket engine while kerosene provides a cost optimised option for the launch vehicle. Methane has intermediate properties between hydrogen and kerosene. In order to obtain good performance at moderate cost, methane has since stood out as a promising option for reusable boosters, main stage and upper stage rocket engines.

The use of methane instead of kerosene solves the problems of soot formation and coking in cooling channels. In addition, methane has cheaper costs in production and storage, and better cooling properties compatible with liquid oxygen due to similar thermodynamic properties [1]. Methane is also a green propellant with low pollution to the environment and is safe to handle and store. The rocket fuel tank size can be reduced due to the high density of methane as compared to hydrogen and a less complicated cooling system can be designed, thus providing more payload mass in return [1]. Therefore, methane is an excellent choice for upper stage and main stage engines. With the increasing interest for Mars return missions, the motivation to use methane becomes prevalent. Studies have suggested that methane is abundant in the Martian atmosphere and possibly under the surface crust [2]. This implies that methane

could be synthesised on Mars to be used for the return mission from Mars as rocket fuel and this, in the future, could enable a manned mission to Mars. For the present work, the rocket operating conditions of both upper stage and main stage rocket engines have been considered.

There are many simplified kinetic models for methane, for example that by Westbrook and Dryer [3], that by Jones and Lindstedt [4] and that by Li and Williams [5]. However, all simplified (reduced) models have been developed for a certain goal and for a certain range of parameters and they are not valid outside this range of parameters. Petersen and co-workers [6] and Zhukov *et al.* [7] studied the ignition of methane–air mixtures at high pressures. They showed that methane oxidation kinetics has its particularities at high pressures. In particular, a new reaction path appears at high pressures *via* the formation of CH_3O_2. Such an important reaction as

$$H + O_2 \rightarrow OH + O \quad (1)$$

gives way to another reaction at high pressures

$$H + O_2 + M \rightarrow HO_2 + M \quad (2)$$

There is a natural trend in methane kinetics at the transition from low pressures to high pressures and from diluted mixtures to pure oxygen mixtures, that is the increased roles of tri-molecular reactions (*i.e.* recombination processes), the formation of peroxy species and the transition to degenerate branching.

For high pressure conditions, there is a reduced methane mechanism due to Petersen and Hanson called REDRAM [8]. This was intended for the modelling of methane ignition at RAM accelerator conditions (https://en.wikipedia.org/wiki/Ram_accelerator) which means pressures above 50 atm, dilution below 70% (*i.e.* the fraction of inert component in the mixture) and fuel-rich mixtures. Thus, these conditions are the nearest to those in rocket combustion chambers. The mechanism was derived from a detailed mechanism of the same research group [6]. The detailed mechanism, called RAMEC, was obtained from an earlier version of the GRI-Mechanism [9] by adding the reactions of peroxy species: CH_3O_2, CH_3O_2H, C_2H_5O, $C_2H_5O_2$ and $C_2H_5O_2H$. The addition of the kinetics of peroxy species improved significantly the agreement of RAMEC with experimental data at high pressures. The reduced (skeletal) mechanism was derived by Petersen and Hanson from RAMEC by systematically eliminating reactions and species that have no influence on the ignition delay time or on the final product temperature (such types of reduced mechanisms are generally referred to as skeletal). The reduction technique was based on a sensitivity analysis.

Zhukov and co-workers developed a detailed kinetic mechanism of oxidation of alkanes from methane to *n*-heptane at high pressures [10,11]. The mechanism was validated at pressures up to 500 atm. The methane sub-mechanism was based on RAMEC [6]. In this work, the mechanism of Zhukov and co-workers [10,11] has been selected as a basis for the new skeletal mechanism because, in contrast to RAMEC, it contains the complete kinetics of propane and ethane derivatives, whose role was not yet clear in methane kinetics under rocket engine conditions, which are the combustion of undiluted fuel–oxygen mixtures at high pressures.

2. MODEL REDUCTION

2.1 General overview

Two types of chemical reactors have been used in the present work to simulate the combustion of methane: a constant pressure adiabatic batch reactor and a counterflow laminar burner. The constant pressure batch reactor has been used to simulate ignition behind shock waves and the counterflow laminar burner has been used to simulate non-premixed flames. These two types of chemical reactors are supposed to be enough to simulate all chemical processes in a rocket combustion chamber. The simulations have been performed with pure methane and oxygen as reagents at a pressure of 60 bar. The calculations have been carried out using the software package Cantera [12].

After narrowing the range of conditions to high pressures and pure methane–oxygen mixtures, the large detailed mechanism by Zhukov and co-workers [10,11] becomes strongly overdetermined. This allows the reduction of the detailed mechanism to a skeletal one. The method used by Peterson and Hanson [8] has a drawback. The sensitivity analysis shows only those processes that are limiting. Alkane oxidation is characterised by degenerate chain branching at high pressures [10,11]. This means that the oxidation of methane occurs as a consequence of reactions where one reaction can be limiting while other reactions are equally important because the formation of final products is impossible without them. That is why the reaction path analysis has been carried out additionally to the sensitivity analysis. The reaction path analysis on its own is insufficient because it is characteristic of chain processes that intermediate species formed in minor quantities may have a strong impact on the rate of chemical processes.

The reduction of the detailed mechanism [10] has been performed in three stages. In the first stage, the reaction path analysis has been done, since it requires less computational resources. Species which are formed in negligible quantities and do not participate in the formation of the final products were eliminated from the mechanism after this stage. In the next stage, a sensitivity analysis has been carried out. It showed reactions that do not exercise influence on the flame temperature and ignition delay time and therefore can be excluded from the mechanism. At the final stage the reduction was performed by the "trial and error" method, which is the most expensive from the point of view of time and effort spent. The hydrogen sub-mechanism has not been analysed and was not considered for the reduction because it was assumed already compact (or well-defined).

The mechanism reduction performed in the present work is (in simple terms) the elimination of species and reactions which are "unnecessary" for the conditions of rocket combustion chambers. Here it is necessary to explain why this reduction cannot be done by simpler methods, without carrying out reaction path and sensitivity analyses, especially since the final result has been obtained using the "trial and error" method. The oxidation of methane occurs in a reaction involving radicals and this is the reason why we cannot use mole fraction as a criterion for the reduction and simply eliminate the species with a small mole fraction in the mixture. Otherwise, we would remove from the mechanism many radicals which have a small mole fraction but are very active. It should be noted that two thirds of the reaction intermediates are radicals. In fact, the fraction of radicals is not large because they have a high rate of consumption due to their reactivity. We also cannot use reaction rate as the criterion, because in sequential processes the limiting reactions are reactions with the lowest rate and

sequential processes are also present in methane oxidation. In order to eliminate "unnecessary" species and reactions, we have analysed by which paths methane is oxidised to CO_2 and which reactions are limiting in these paths.

2.2 Reaction path analysis

The reaction path analysis consisted of determination of the amount of species containing a carbon atom formed from one mole of methane under certain conditions. It shows the major pathways in the premixed stoichiometric methane–oxygen mixture for temperatures from 1000 up to 3000 K at high pressures as follows

$$CH_4 \rightarrow CH_3 \rightarrow CH_3O \rightarrow CH_2O \rightarrow HCO \rightarrow CO \rightarrow CO_2 \quad (3)$$

$$CH_4 \rightarrow CH_3 \rightarrow C_2H_6 \rightarrow C_2H_5 \rightarrow C_2H_4 \rightarrow C_2H_3 \quad (4)$$

The reaction path analysis shows the importance of the C2 mechanism as the main alternative reaction pathway. The reactions with methanol (CH_3OH) and hydroxymethyl (CH_2OH) leading up to formaldehyde (CH_2O) are in low net flux and indicate a low production rate of these species during combustion under the present conditions. CH_3O, CH_2O, and HCO are important intermediate species for methane combustion and are included in the final skeletal mechanism. The analysis shows also the formation of C3 species, but their net flux amounts to about 1%. At higher temperatures (> 3000 K), the reaction pathways shift after CH_3 from CH_3O and C_2H_6 to CH_2O and CH_2.

In the case of non-premixed flames, the reaction pathways are determined by the position relative to the flame front. On the part of the flame which is facing to the oxygen inflow, the H–O kinetics dominate. The C–O kinetics are represented only by the last stage of methane oxidation

$$CO \rightarrow CO_2 \quad (5)$$

On the fuel-rich side, the formation of C2 species is the main reaction pathway

$$CH_4 \rightarrow CH_3 \rightarrow C_2H_5 \rightarrow C_2H_4 \rightarrow C_2H_3 \rightarrow C_2H_2 \quad (6)$$

The formation of a large amount of ethane and its derivatives is natural at this location due to the high rate of CH_3 production with the lack of oxygen. However, the further formation of C3 and C4 species through the recombination of CH_3, C_2H_5 and other radicals is less pronounced. The amount of C3 species formed in the flame front is dozens of times less in comparison with the C2 species.

The most complex pattern of the reaction pathways is observed in the middle of the non-premixed flame, in the region where the local stoichiometry is close to unity and the temperature and heat release reach their maximum. The corresponding reaction-path diagram is presented in Figure 1. However, the diagram does not have any new reaction pathways with respect to the results already mentioned.

Summing up the results of the reaction path analysis, we can conclude that C3 and heavier species do not play a significant role in the combustion of methane–oxygen mixtures at high pressures. Based on the results of the analysis of the reaction pathways, the reduction of the detailed mechanism by Zhukov [11] was carried out. For the reduction, the truncated version of the detailed mechanism [10] was used, which contains species not larger than C4 and consists of

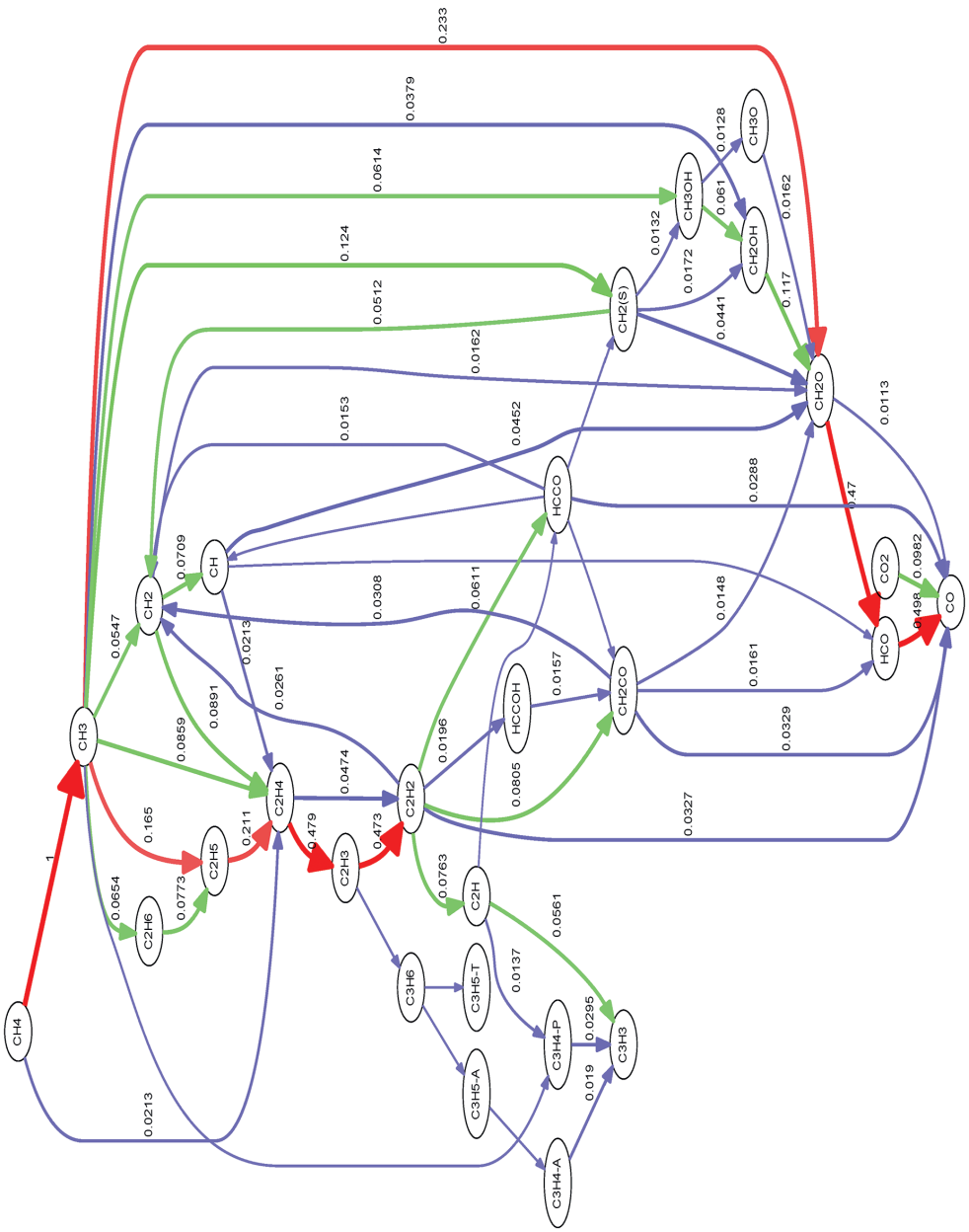

Figure 1 Reaction path diagram in the middle of non-premixed methane–oxygen flame at 60 bar.

1260 reactions and 207 species. At first, all C3 and C4 species have been eliminated. The initial hypothesis, that they might play a role in methane kinetics under rocket engine conditions, was not confirmed. As we saw, C4 species are formed in negligible amounts in CH_4/O_2 flames and the amount of the C3 species is too small. The hypothesis is not substantiated, because the transition to rocket engine conditions means not only high pressures but also high temperatures reduce the role of recombination processes. At the next step, the oxygenated C2 species, which are also not involved in the major reaction pathways, were removed. The obtained skeletal mechanism has the working name ReduceRXN and consists of 165 reactions and 26 species.

The reaction path analysis allowed us to identify which species are the most important under rocket engine conditions and gave us the opportunity to reduce the mechanism to a reasonable size. However, the reaction path analysis does not show the impact of separate reactions and also does not allow one to eliminate "unnecessary" reactions. To solve this task, a sensitivity analysis was carried out.

2.3 Sensitivity analysis

A sensitivity analysis has been carried out to determine the rate-limiting reaction steps of the kinetic mechanism ReduceRXN. For this purpose, sensitivity coefficients S_r of current temperature to reaction rates were calculated, which are defined as follows

$$S_r = \frac{k_r}{T}\frac{\partial T}{\partial k_r} \tag{7}$$

where k_r is a reaction rate of reaction r and temperature T is taken at some point in time or in space. In the present work, the sensitivity coefficients were calculated at the point of ignition (the highest time derivative of temperature), since they reach their maximum values at that moment. The coefficients were calculated for a stoichiometric CH_4–O_2 mixture in an adiabatic constant pressure reactor at a pressure of 60 bar for a wide range of initial temperatures from 800 to 2100 K. Ignition of the CH_4–O_2 mixture occurs as a chain-thermal explosion under these conditions, so the sensitivity to temperature of a particular reaction adequately describes the contribution of the reaction to the mixture reactivity. Sensitivity coefficients S_r can be calculated not only with regard to temperature but also with regard to other parameters, for example, ignition delay time τ. In this case, temperature T should be replaced by another variable or parameter in Eqn (7). In ref. [10], it was shown that the time integrals of $S_r(T)$ from zero to the time of ignition are proportional to the sensitivity coefficients for ignition delay times.

As for the counterflow flame, in order to get a comprehensive view of the kinetics, the sensitivity coefficients were calculated at three different locations: on the rich side of the flame, on the lean side of the flame and in the middle of the flame, where the temperature reaches its maximum. However, the sensitivity coefficients calculated at T_{max} (maximum temperature point) were primarily taken into account. Flame temperature (or T_{max}) is the objective parameter for the reduced mechanism; thus, coefficients $S_r(T_{max})$ directly characterise the importance of a particular reaction.

The sensitivity analysis demands significantly more computations than the reaction path analysis. Besides post-processing, the sensitivity analysis requires one to perform simulations of ignition or flame twice for each reaction. Therefore, the sensitivity analysis has been done after the reaction path analysis and the preliminary reduction of the original mechanism. Figures 2 and 3 present the results of the sensitivity analysis for the stoichiometric methane–oxygen mixture in a constant pressure batch reactor and in a counterflow flame at a pressure of 60 bar.

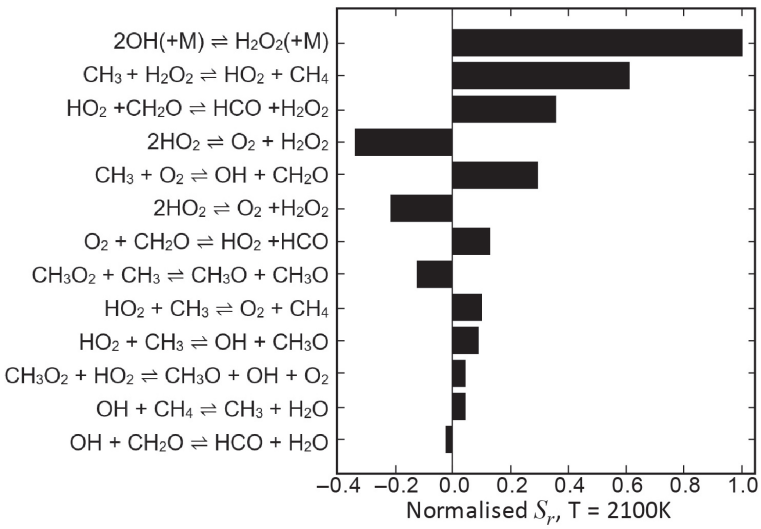

Figure 2 Sensitivity coefficients during the ignition of methane–oxygen mixture at 60 bar and 2100 K.

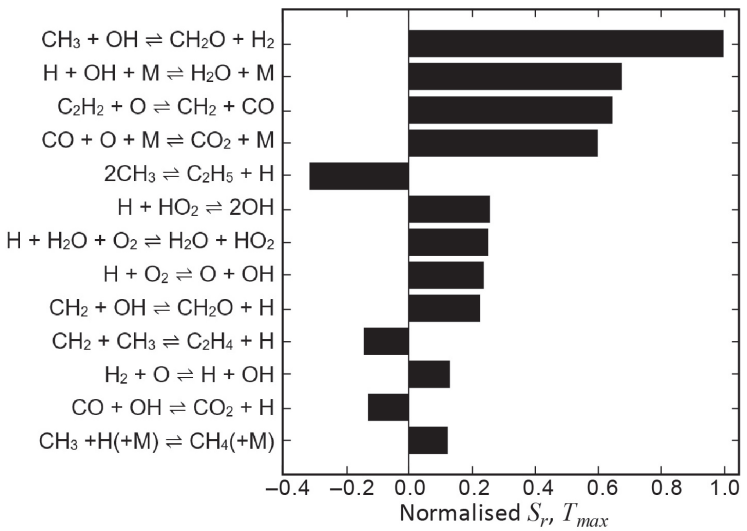

Figure 3 Sensitivity coefficients in the middle of non-premixed methane–oxygen flame at 60 bar.

The first 13 reactions with the highest S_r are only shown in the figures (reaction $2HO_2 \rightleftharpoons O_2 + H_2O_2$ has a dual-exponential fit, *i.e.* is presented as duplicate reactions). For ease of reference, the sensitivity coefficients were normalised to the largest sensitivity coefficient. The sensitivity analysis was carried out for all 165 reactions in ReduceRXN and also under other conditions. However, the reactions shown in Figures 2 and 3 have the greatest importance under rocket engine conditions.

The analysis showed that the reactivity of the mixture is highly sensitive to the reactions involving hydroperoxy radical (HO_2) and hydrogen peroxide (H_2O_2) during ignition of methane at elevated pressures (see Figure 2). This is due to the fact that the HO_2 formation rate increases

with pressure and becomes, at high pressures, higher than the rates of formation of radicals OH and O. The sensitivity analysis also shows that the kinetics of the premixed methane–oxygen mixture are sensitive to CH_3O_2 at high pressures.

The important reactions in the counterflow flame (see Figure 3) are vastly different from those of the ignition of the premixed mixture in a batch reactor (see Figure 2). The main distinctive feature of the kinetics of non-premixed methane–oxygen flames at high pressures is the relatively large contribution of C2 species. The sensitivity analysis of the counterflow flame has been performed not only in the middle of the flame but also on fuel and oxidiser sides of the flame. The sensitivity coefficients in a constant pressure batch reactor have also been calculated at different temperatures. However, these results do not add anything worthy of attention to the results already obtained.

The sensitivity analyses in a constant pressure batch reactor and in a counterflow flame have shown that up to 33 reactions along with three species contribute little effect to the ignition delay times and temperature profile in counterflow flames. Following the results of the sensitivity analysis, the species C_2H_2, $CH_2(S)$ (singlet methylene) and CH were eliminated from the mechanism.

In contrast to the reaction path analysis, the sensitivity analysis gave the ranking of the reactions but not of species. It allowed the elimination of reactions with very low sensitivity coefficients, which obviously do not play a role at all under the conditions considered. However, the performed sensitivity analysis shows the effect at small changes of reaction rate constants and gives no idea what will happen if a particular reaction is completely removed. Thus, the extent to which reactions can be eliminated can only be found using a “trial and error” or "cut and try" method.

2.4 “Cut and try” method

After the two stages of the reduction, it was found that the difference in simulation results between the reduced and parent detailed mechanisms is invisible. This indicated that the reduced mechanism was still overdetermined and there was potential for further reduction. The initial objective of the reduction was to obtain the skeletal mechanism that gives acceptable predictions of ignition delay times and predicts flame temperatures under rocket engine conditions within 2% margins relative to the original detailed mechanism. The overdetermination occurs as a result of the very conservative criteria used for eliminating the “unnecessary” reactions. Both species flows and sensitivity coefficients are not absolute values but are normalised to the maximum value of species flow or to the maximum value of sensitivity coefficients. The elimination of minor reaction pathways leads to the redistribution of flows on major reaction pathways. Therefore, the elimination of the species and reactions with flows and sensitivity coefficients of about 0.05 did not lead to a visible difference between the detailed and reduced mechanisms.

For the further reduction, the “cut and try” method was employed. This method is the most costly from the point of view of time spent; thus, its application has sense only in the final stage when the kinetic mechanism is already established. The method used was based on the results of the sensitivity analysis and it is a continuation of the previously used reduction technique. In contrast to the previously used method, the reactions were not eliminated by one large group at this stage but individually where the reaction with the smallest sensitivity coefficients was removed first. The comparison with the detailed

mechanism and experimental data was performed not at the end of the work but after each try. The elimination of reactions was repeated iteratively until the truncation of the reaction

$$CH_3 + HCO \rightleftharpoons CH_4 + CO \quad (8)$$

noticeably altered the temperature profile in the non-premixed counterflow flame of the methane–oxygen mixture at a pressure of 60 bar. Thus, reaction (8) is the reaction with the lowest sensitivity coefficients left in the mechanism.

The "cut and try" method resulted in the mechanism consisting of 23 species and 51 reversible reactions (depending on the counting rule for duplicate reactions and for three-body reactions, the size of the final reduced mechanism can be smaller or larger). The final version of the reduced mechanism is labelled on graphs as ReduceSens. It is provided in CHEMKIN format in Appendix A. The mechanism in CHEMKIN format, together with transport and thermodynamic properties, is also available by email upon request to the corresponding author.

With this method, the potential for the "simple" reduction of the detailed mechanism has been exhausted. Any further reduction of the methane mechanism requires other methods.

3. VERIFICATION AND VALIDATION OF SKELETAL MECHANISM

Two mechanisms, one from the reduction by reaction path analysis, ReduceRXN and the final developed skeletal mechanism, ReduceSens, have been validated against two sets of experimental data at 50 atm (Figure 4). The experimental data comes from a shock tube experiment done by Petersen *et al.* [13] and by Zhukov *et al.* [7] and consisted of ignition delay

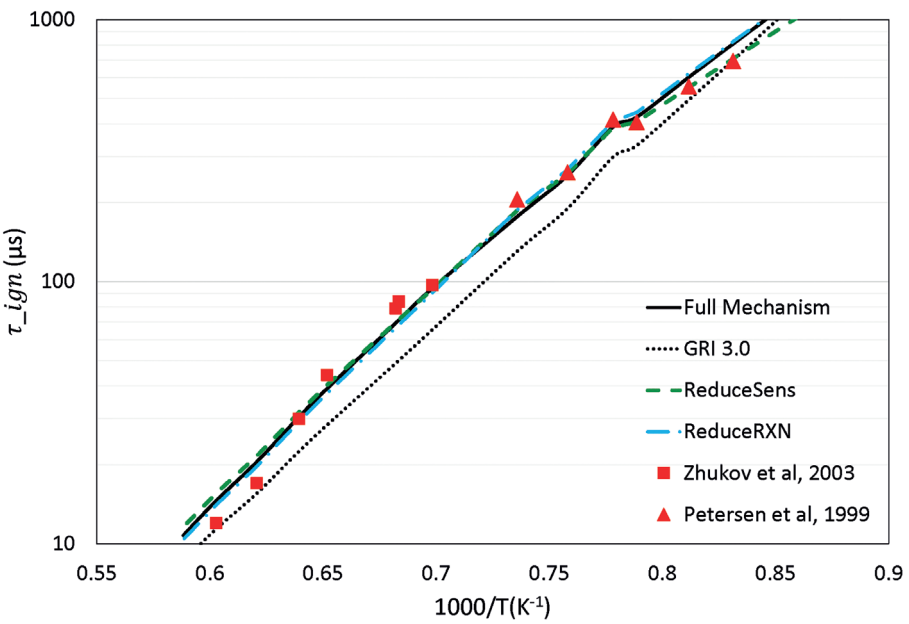

Figure 4 Calculated ignition delay times in comparison with experimental data: p = 50 atm, lean methane–air mixture.

times measured at highly elevated pressure of more than 40 bar. Petersen *et al.* [13] investigated the ignition delay times for CH_4/O_2/diluent at ϕ = 0.4, 3.0 and 6.0 (ϕ is equivalence ratio) using either N_2, Ar or He as diluent gas. Zhukov *et al.* [7] investigated the ignition delay time for methane–air mixtures at ϕ = 0.5 and at pressures up to 450 atm. These two experiments were chosen for validation as they are the closest to rocket engine conditions. Figure 4 shows that both ReduceSens and ReduceRXN are in good agreement with the full mechanisms and experimental data, with ReduceSens having a better fit to experimental data. Both ReduceSens and ReduceRXN are therefore within the desired error range of 5%.

As a comparison, the most widely used mechanism GRI-Mech 3.0 [14] is plotted. It was shown [6,7] that GRI-Mech 3.0 could not be used at high pressures (≥ 50 atm) due to the fact that it does not contain species such as CH_3O_2 that are important for low temperature and high pressure conditions. It is also worth mentioning that the pressures of about 60 bar exceed significantly the validity range of GRI-Mech 3.0 (10 Torr to 10 atm) [14]. Furthermore, it was found [15] that the lower the diluent fraction is in the mixture, the lower is the accuracy of GRI-Mech 3.0. Thus, GRI-Mech 3.0 should not be used for rocket engine conditions.

Due to the unavailability of experimental data for undiluted (pure methane–oxygen) mixtures, the new skeletal model cannot be validated under rocket engine-relevant conditions. However, the skeletal and reduced models can be verified under these conditions against the parent detailed mechanism by Zhukov and co-workers [10,11]. Figure 5 shows the comparison of the skeletal mechanisms with other methane mechanisms under rocket engine-relevant conditions: p = 60 bar and a stoichiometric methane–oxygen mixture. The results from the REDRAM kinetic mechanism [8] are also plotted to test the capability of the mechanism under rocket engine conditions. GRI-Mech 3.0 is also shown for comparison. Presently,

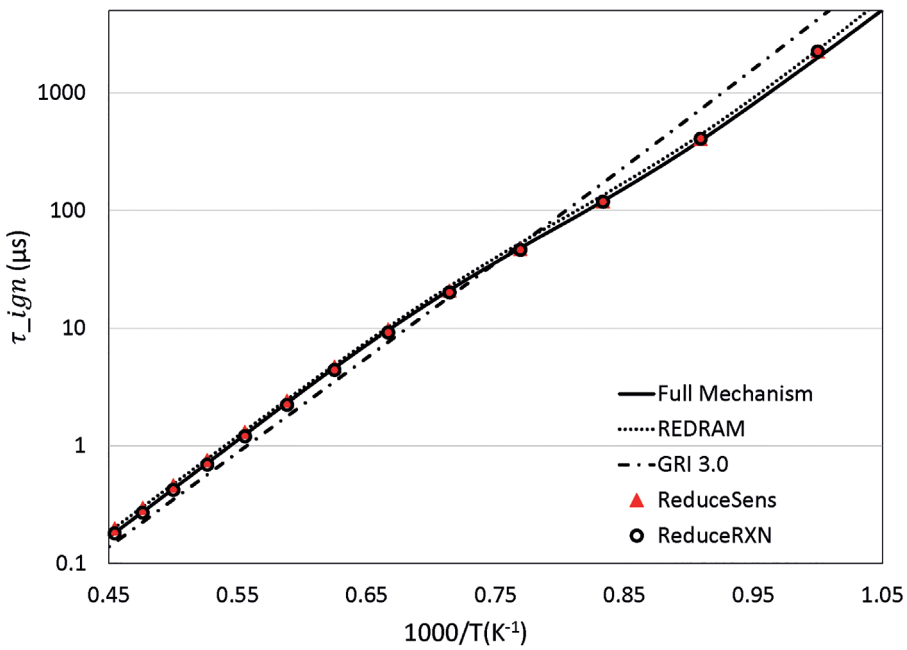

Figure 5 Comparison of different mechanisms under rocket engine-relevant conditions: p = 60 bar, stoichiometric methane–oxygen mixture.

there are no data available in the literature from shock tube experiments under conditions similar to the rocket engine conditions, since all experiments have been done with either air as oxidiser or with an oxygen mixture diluted with an inert gas such as nitrogen or argon. The final skeletal mechanism gives ignition delay times within 5% error from the parent detailed mechanism. From Figure 5 it follows that the reduced mechanisms REDRAM, ReduceSens and ReduceRXN have the same accuracy in the prediction of ignition delay times when compared with the parent detailed mechanism.

The developed mechanism has been also verified with the temperature profile for the counterflow flame. As a comparison, the results obtained using REDRAM [8] are plotted (see Figure 6). The results obtained from the Jones–Lindstedt mechanism [4] are also included to compare the performance between a skeletal mechanism of 51 reactions and a reduced mechanism of four reactions. The Jones–Lindstedt mechanism was selected as it is widely used in many computational fluid dynamics simulations of methane combustion. Both REDRAM and Jones–Lindstedt mechanisms perform poorly in the case of non-premixed combustion under rocket engine conditions. The peak temperature is underpredicted, with an error value up to 1500 K.

The Jones–Lindstedt mechanism [4] does not contain OH, O and H radicals and thus less heat release was accounted for in the formation and recombination of such radicals. The predicted peak temperature is thus much lower. For REDRAM, the skeletal mechanism was developed using ignition delay times as criteria and the validation was carried out only for the ignition of premixed mixtures [8]. Hence, the resultant mechanism contains fewer reactions to account for fuel-rich combustion and the predicted peak temperature is lower by 500 K. This stresses the importance of correctly identifying the appropriate simulation

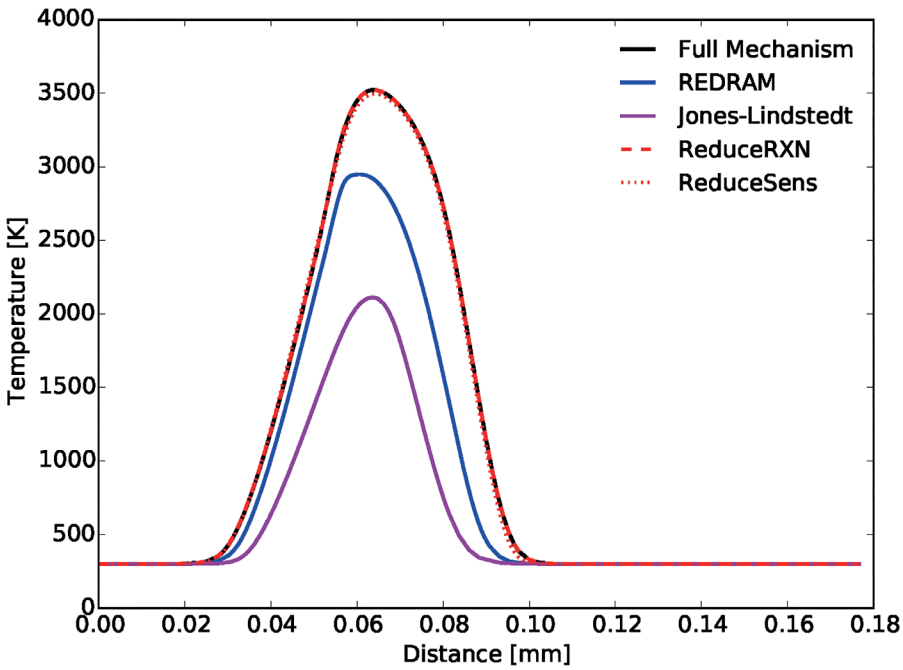

Figure 6 Simulated temperature profiles in counterflow methane–oxygen flame at 60 atm.

conditions, which represent the desired application environment for a reduced model, since this greatly influences which reactions to eliminate and which to keep. From Figure 6, both ReduceSens and ReduceRXN are in good agreement with the parent detailed mechanism. No comparison with experimental data has been done for the counterflow flame as there is no available experimental data at pressures above 10 atm. This suggests that more work needs to be done to obtain validation data for the developed kinetic mechanism. As a secondary verification, the comparison by species profiles of CH_4, O_2, CO_2, H_2O, CO and OH was performed. The same observation can be made with the accuracy of the Jones–Lindstedt and REDRAM mechanisms for predicting these species' mole fractions. Both ReduceSens and ReduceRXN perform well in predicting the species profile within 5% error of the full mechanism with a larger error seen in the prediction of CO and OH radicals, which is not critical for the simulations of rocket combustion chambers. The lower concentration, by 12%, of CO in non-premixed counterflow flames is the main distinction of the new skeletal mechanism, in terms of performance, from the parent detailed mechanism.

By reducing the size of the full mechanisms by around 25 times, the computation time has been reduced by a similar amount. The benefit of the reduction is more pronounced for the counterflow flame simulation where the computation time is reduced by two orders of magnitude. If the use of the mechanism were to be extended to 2D and 3D simulations, with hundreds of grid cells to solve, the advantage of having a smaller size mechanism would quickly become obvious.

4. CONCLUSIONS

The skeletal mechanism of 23 species and 51 reactions was developed from the detailed mechanism of Zhukov *et al*. [10], which consists of 1260 reactions and 207 species. Two of the species in the reduced mechanism are neutral diluents: N_2 and Ar, which can be omitted in pure methane–oxygen mixtures.

The reduction of the detailed mechanism was done using the results of reaction path analysis and sensitivity analysis, which were carried out in a constant pressure batch reactor and in a counterflow flame at a pressure of 60 bar for pure methane–oxygen mixtures. The reaction path analysis showed the species that are important under rocket combustion conditions. The sensitivity analysis gave the ranking of the reactions according to their impact on gas temperature during ignition and in non-premixed flame. The developed mechanism was shown to perform well in the predictions of ignition delay times and of temperature profile for counterflow flame under rocket operating conditions. The predicted values of temperature are on average within 1% error from the parent detailed mechanism.

C3 and C4 species are found to be insignificant in methane combustion under rocket operating conditions. The reaction path analysis in a constant pressure batch reactor and in a counterflow flame shows that species such as C, CH_3O_2H, CH_3OH, CH_2OH, HCO_2, HCO_3 and HCO_3H are formed in minor amounts and thus do not influence ignition delay times and the temperature profile of counterflow flames at high pressures. The C2 sub-mechanism consisting of C_2H_6 to C_2H_3 is considered important for fuel-rich combustion of methane. However, the other C2 oxy species are found to be unimportant for rocket-relevant conditions.

5. ACKNOWLEDGEMENTS

The present work was conducted in the framework of the German Aerospace Centre (DLR) project TAUROS (TAU for Rocket Thrust Chamber Simulation) focusing on the qualification and advancement of the DLR flow solver TAU for liquid rocket thrust chamber applications. The financial support of the DLR Space Research Programme is highly appreciated. The results of this work were presented at the 8th European Combustion Meeting in Dubrovnik, Croatia, April 2017.

6. APPENDIX A: FINAL VERSION OF THE REDUCED MECHANISM IN 'CHEMKIN' FORMAT

```
ELEMENTS

H C O N AR

END

SPECIES

H2      H       O       O2      OH      H2O     HO2     H2O2

CH2     CH3     CH4     CO      CO2     HCO     CH2O    CH3O

C2H3    C2H4    C2H5    C2H6    CH3O2   N2      AR

END

REACTIONS      CAL/MOLE

O2+CH2O<=>HO2+HCO                       1.000E+14    0.000  40000.00

H+O2+M<=>HO2+M                          2.800E+18   -0.860      0.00

O2/0.00/ H2O/0.00/ CO/0.75/ CO2/1.50/ C2H6/1.50/ N2/0.00/ AR/0.00/

H+2O2<=>HO2+O2                          3.000E+20   -1.720      0.00

H+CH2O(+M)<=>CH3O(+M)                   5.400E+11    0.454   2600.00

     LOW  /  2.200E+30   -4.800   5560.00/

     TROE/  0.7580   94.00  1555.00  4200.00 /

H2/2.00/ H2O/6.00/ CH4/2.00/ CO/1.50/ CO2/2.00/ C2H6/3.00/

2OH(+M)<=>H2O2(+M)                      7.400E+13   -0.370      0.00

     LOW  /  2.300E+18   -0.900  -1700.00/

     TROE/  0.7346   94.00  1756.00  5182.00 /
```

```
H2/2.00/ H2O/6.00/ CH4/2.00/ CO/1.50/ CO2/2.00/ C2H6/3.00/ AR/0.70/
OH+HO2<=>O2+H2O                          2.900E+13    0.000   -500.00
OH+H2O2<=>HO2+H2O                        1.750E+12    0.000    320.00
 DUPLICATE
OH+H2O2<=>HO2+H2O                        5.800E+14    0.000   9560.00
 DUPLICATE
OH+CH4<=>CH3+H2O                         1.000E+08    1.600   3120.00
2HO2<=>O2+H2O2                           1.300E+11    0.000  -1630.00
 DUPLICATE
2HO2<=>O2+H2O2                           4.200E+14    0.000  12000.00
 DUPLICATE
HO2+CH3<=>O2+CH4                         1.000E+12    0.000      0.00
HO2+CH3<=>OH+CH3O                        2.000E+13    0.000      0.00
HO2+CO<=>OH+CO2                          1.500E+14    0.000  23600.00
HO2+CH2O<=>HCO+H2O2                      1.000E+12    0.000   8000.00
CH3+O2<=>O+CH3O                          2.675E+13    0.000  28800.00
CH3+O2<=>OH+CH2O                         3.600E+10    0.000   8940.00
CH3+H2O2<=>HO2+CH4                       2.450E+04    2.470   5180.00
CH3+CH2O<=>HCO+CH4                       3.320E+03    2.810   5860.00
CH3O+HO2<=>CH2O+H2O2                     1.200E+13    0.000      0.00
CH3O2+CH3<=>CH3O+CH3O                    3.000E+13    0.000  -1200.00
CH3O+O2<=>HO2+CH2O                       4.280E-13    7.600  -3530.00
CH3+O2<=>CH3O2                           1.700E+60  -15.100  18785.00
CH3O+CH3<=>CH2O+CH4                      2.410E+13    0.000      0.00
O+CH4<=>OH+CH3                           1.020E+09    1.500   8600.00
```

```
H+O2<=>O+OH                                 8.300E+13    0.000  14413.00

H+O2+H2O<=>HO2+H2O                          9.380E+18   -0.760      0.00

O+H2<=>H+OH                                 5.000E+04    2.670   6290.00

O+CH3<=>H+CH2O                              8.430E+13    0.000      0.00

O+CO+M<=>CO2+M                              6.020E+14    0.000   3000.00

H2/2.00/ O2/6.00/ H2O/6.00/ CH4/2.00/ CO/1.50/ CO2/3.50/ C2H6/3.00/
AR/0.50/

H+OH+M<=>H2O+M                              2.200E+22   -2.000      0.00

H2/0.73/ H2O/3.65/ CH4/2.00/ C2H6/3.00/ AR/0.38/

H+CH3(+M)<=>CH4(+M)                         1.270E+16   -0.630    383.00

     LOW  /  2.477E+33   -4.760   2440.00/

     TROE/  0.7830   74.00  2941.00  6964.00 /

H2/2.00/ H2O/6.00/ CH4/2.00/ CO/1.50/ CO2/2.00/ C2H6/3.00/ AR/0.70/

H+HCO(+M)<=>CH2O(+M)                        1.090E+12    0.480   -260.00

     LOW  /  1.350E+24   -2.570   1425.00/

     TROE/  0.7824  271.00  2755.00  6570.00 /

H2/2.00/ H2O/6.00/ CH4/2.00/ CO/1.50/ CO2/2.00/ C2H6/3.00/ AR/0.70/

H+C2H4(+M)<=>C2H5(+M)                       1.080E+12    0.454   1820.00

     LOW  /  1.200E+42   -7.620   6970.00/

     TROE/  0.9753  210.00   984.00  4374.00 /

H2/2.00/ H2O/6.00/ CH4/2.00/ CO/1.50/ CO2/2.00/ C2H6/3.00/ AR/0.70/

H+C2H4<=>C2H3+H2                            1.325E+06    2.530  12240.00

H+C2H6<=>C2H5+H2                            1.150E+08    1.900   7530.00

OH+H2<=>H+H2O                               2.160E+08    1.510   3430.00

OH+CH2<=>H+CH2O                             2.000E+13    0.000      0.00

OH+C2H6<=>C2H5+H2O                          3.540E+06    2.120    870.00
```

```
HCO+O2<=>HO2+CO                          7.600E+12    0.000    400.00

HCO+M<=>H+CO+M                           1.870E+17   -1.000  17000.00

H2/2.00/ H2O/12.0/ CH4/2.00/ CO/1.50/ CO2/2.00/ C2H6/3.00/

CH3+OH<=>CH2O+H2                         8.000E+12    0.000      0.00

CH2+CH3<=>H+C2H4                         4.000E+13    0.000      0.00

O2+CO<=>O+CO2                            2.500E+12    0.000  47800.00

OH+CO<=>H+CO2                            4.760E+07    1.228     70.00

OH+CH2O<=>HCO+H2O                        3.430E+09    1.180   -447.00

H+CH2O<=>HCO+H2                          2.300E+10    1.050   3275.00

H+CH4<=>CH3+H2                           6.600E+08    1.620  10840.00

2CH3(+M)<=>C2H6(+M)                      2.120E+16   -0.970    620.00

     LOW  /  1.770E+50   -9.670   6220.00/

     TROE/  0.5325  151.00  1038.00  4970.00 /

H2/2.00/ H2O/6.00/ CH4/2.00/ CO/1.50/ CO2/2.00/ C2H6/3.00/ AR/0.70/

H+O2+N2<=>HO2+N2                         2.600E+19   -1.240      0.00

H+O2+AR<=>HO2+AR                         7.000E+17   -0.800      0.00

END
```

Published online: 28 February 2018

7. REFERENCES

[1] Burkhardt, H., Sippel, M., Herbertz, A. and Klevanski, J. (2004) *J. Spacecr. Rockets*, **41**, 762–769.
[2] Webster, C.R., Mahaffy, P.R., Atreya, S.K. *et al.* (2015) *Science*, **347**, 415–417.
[3] Westbrook, C.K. and Dryer, F.L. (1981) *Combust. Sci. Technol.*, **27**, 31–43.
[4] Jones, W.P. and Lindstedt, R.P. (1988) *Combust. Flame*, **73**, 233–249.
[5] Li, S.C. and Williams F.A. (2002) *J. Eng. Gas Turbines Power*, **124**, 471–480.
[6] Petersen, E.L., Davidson, D.F. and Hanson, R.K. (1999) *Combust. Flame*, **117**, 272–290.
[7] Zhukov, V.P., Sechenov, V.A. and Starikovskii, A.Y. (2003) *Combust., Explos. Shock Waves (Engl. Transl.)*, **39**, 487–495.
[8] Petersen, E.L. and Hanson, R.K. (1999) *J. Propul. Power*, **15**, 591–600.
[9] Frenklach, M., Wang, H., Yu, C.L. *et al.* (1995) *GRI-Mech-An optimized detailed chemical reaction mechanism for methane combustion,* report No. GRI-95/0058. Gas Research Institute, USA.

[10] Zhukov, V.P., Sechenov, V.A. and Starikovskii, A.Y. (2005) *Kinet. Catal.*, **46**, 319–327.
[11] Zhukov, V.P. (2009) *Combust. Theory Modell.*, **13**, 427–442.
[12] Goodwin, D.G., Moffat, H.K. and Speth, R.L. (2015) *Cantera: an object-oriented software toolkit for chemical kinetics, thermodynamics and transport processes,* http://www.cantera.org
[13] Petersen, E.L., Davidson, D.F. and Hanson, R.K (1999) *J. Propul. Power*, **15**, 82–91.
[14] Smith, G.P., Golden, D.M., Frenklach, M. *et al. GRI–Mech 3.0*, http://www.me.berkeley.edu/gri_mech/
[15] Donohoe, N., Heufer, A., Metcalfe, W.K. *et al.* (2014) *Combust. Flame*, **161**, 1432–1443.